HHS Public Access

Author manuscript

J Control Release. Author manuscript; available in PMC 2022 March 10.

Published in final edited form as:

J Control Release. 2021 March 10; 331: 260–269. doi:10.1016/j.jconrel.2021.01.026.

Delivery of Eupenifeldin via Polymer-Coated Surgical Buttresses Prevents Local Lung Cancer Recurrence

Zeinab Y. Al Subeh[a,§], **Ngoc-Quynh Chu**[b,§], **Jeremy T. Korunes-Miller**[c], **Lillian L. Tsai**[b], **Tyler N. Graf**[a], **Yin P. Hung**[b], **Cedric J. Pearce**[d], **Mark W. Grinstaff**[c,e], **Aaron H. Colby**[c,f,*], **Yolonda L. Colson**[b,*], **Nicholas H. Oberlies**[a,*]

[a]Department of Chemistry and Biochemistry, University of North Carolina at Greensboro, Greensboro, North Carolina 27402, United States

[b]Division of Thoracic Surgery, Massachusetts General Hospital, Boston, Massachusetts 02114, United States

[c]Department of Biomedical Engineering, Boston University, Boston, Massachusetts 02215, United States

[d]Mycosynthetix, Inc., Hillsborough, North Carolina 27278, United States

[e]Department of Chemistry, Boston University, Boston, Massachusetts 02215, United States

[f]Ionic Pharmaceuticals, LLC, Brookline, Massachusetts 02445, United States

Abstract

[*]Corresponding authors: Nicholas H. Oberlies (nicholas_oberlies@uncg.edu), Aaron H. Colby (acolby@bu.edu), Yolonda L. Colson (ycolson@mgh.harvard.edu).

[§]Co-first authors

Credit Author Statement:
Zeinab Y. Al Subeh: Conceptualization, Writing, Formal analysis, Visualization, Investigation
Ngoc-Quynh Chu: Formal analysis, Visualization, Investigation
Jeremy T. Korunes-Miller: Formal analysis, Visualization, Investigation
Lillian L. Tsai: Formal analysis, Visualization, Investigation
Tyler N. Graf: Validation
Yin P. Hung: Formal analysis
Cedric J. Pearce: Resources, Funding acquisition
Mark W. Grinstaff: Conceptualization, Writing, Supervision, Funding acquisition
Aaron H. Colby: Conceptualization, Writing, Visualization, Funding acquisition
Yolonda L. Colson: Conceptualization, Writing, Supervision, Funding acquisition
Nicholas H. Oberlies: Conceptualization, Writing, Supervision, Funding acquisition

Conflict of Interest
AHC and MWG have ownership interest in Ionic Pharmaceuticals, LLC. NHO is a member of the Scientific Advisory Board of Mycosynthetix, Inc.

Appendix A. Supplementary data
Eupenfeldin ^{1}H NMR spectrum and structure of eupenifeldin, UPLC chromatogram of eupenifeldin, solubility of eupenifeldin in PBS solutions with various concentrations of Tween 80, the amount of eupenifeldin released in different volumes of PBS solutions, SEM images of the formulations **1**-**6**, the timeline of the *in vitro* release study, calibration curves along with their precision and accuracy measures, eupenifeldin growth inhibition effect in disease-oriented human tumor cell line panel, IC_{50} values of eupenifeldin against LLC and human A549 cell lines, *in vivo* dose titration study of “free” eupenifeldin, and *in vivo* dose titration study of eupenifeldin-loaded buttress.

Lung cancer is the leading cause of cancer deaths worldwide. Unfortunately, high recurrence rates and poor survival remain despite surgical resection and conventional chemotherapy. Local drug delivery systems are a promising intervention for lung cancer treatment with the potential for improved efficacy with reduced systemic toxicity. Here, we describe the development of a chemotherapy-loaded polymer buttress, to be implanted along the surgical margin at the time of tumor resection, for achieving local and prolonged release of a new anticancer agent, eupenifeldin. We prepared five different formulations of buttresses with varying amounts of eupenifeldin, and additional external empty polymer coating layers (or thicknesses) to modulate drug release. The *in vitro* eupenifeldin release profile depends on the number of external coating layers with the formulation of the greatest thickness demonstrating a prolonged release approaching 90 days. Similarly, the long-term cytotoxicity of eupenifeldin-loaded buttress formulations against murine Lewis lung carcinoma (LLC) and human lung carcinoma (A549) cell lines mirrors the eupenifeldin release profiles and shows a prolonged cytotoxic effect. Eupenifeldin-loaded buttresses significantly decrease local tumor recurrence *in vivo* and increase disease-free survival in a resection model.

Keywords

Local Drug Delivery; Surgical Buttress; Eupenifeldin; Lung Cancer; Polymer; Cancer Recurrence; Prolonged-Release

1. Introduction

Lung cancer is the most common cancer in the world with a projected 1.9 million new cases in 2020 [1, 2]. Despite improvements in prevention, diagnosis, and treatment, lung cancer still has the highest incidence and mortality rate, with nearly 1.8 million deaths in 2018, accounting for more than those reported for breast, colon, and prostate cancers combined [3]. Unfortunately, the overall 5-year relative survival rate for patients with lung cancer is less than 20% [4].

Treatment of lung cancer is usually based on its histological type (non-small cell vs small cell) and stage of the disease, and includes surgical intervention, chemotherapy and radiation, or a combination of these modalities [5]. Surgical resection of primary non-small cell lung cancer (NSCLC) is done with curative intent for stage I-III. Unfortunately, cure decreases as a function of increasing stage with 5-year survival following surgical resection remaining as low as 68% for clinical stage I, 53–60% for stage II, and 13–36% for stage III [6]. Recurrence is attributed, at least in part, to microscopic cancerous cells remaining after tumor resection [7]. The presence of positive surgical margins is a known risk factor for poor prognosis and reduced survival as evidenced by a significant reduction in the 5-year disease-free survival rate among lung cancer patients with positive surgical margins compared to those with clean margins (30.8% vs. 82.6%, $P = 0.001$; Fig. 1A, bottom path) [8, 9].

The high recurrence rate of lung cancer remains a major clinical challenge, and current attempts to prevent potential recurrence with adjuvant systemic chemotherapy are not justified given the associated toxicity [10]. For example, the International Adjuvant Lung Cancer Trial (IALT) showed that adjuvant cisplatin-based chemotherapy following complete

resection of NSCLC lead to a 4% increase in 5-year survival and a 5% higher disease-free survival rate in patients but, similar to other trials, did not significantly prevent nodal or local recurrence [11–14]. Furthermore, systemic administration of chemotherapies carries the potential for both off-target toxicities and side effects that are typically not justified by the limited efficacy [15]. Consequently, there is a need for innovative approaches for eliminating residual cancer cells after surgery, particularly approaches with reduced toxicity, and with a particular emphasis on treating NSCLC.

Successful approaches to address these challenges require the development of drug delivery systems that target cancerous cells in the lung with minimal effects on normal tissues. One strategy to achieve this goal is to use nanoscale drug carriers synthesized from versatile materials, such as polymers [16–20], lipids [21, 22], or inorganic carriers [23], to selectively deliver an anticancer agent to the tumor site. However, these strategies suffer from a lack of tumoral accumulation and drug delivery in much the same way as systemic chemotherapy. As an alternative strategy, we are investigating the delivery of therapeutics via surgical buttresses that are implanted at the resection margin at the time of surgery, providing a locally high dose of chemotherapy for a prolonged period while averting systemic toxicity (Fig. 1A, top path). Coating a standard surgical buttress with polymer-drug formulations yields a flexible, conformal, biocompatible device that is easily handled and implanted. Various types of “unloaded” buttresses are clinically available and can be employed to reinforce the lung tissue at the resection margin in order to prevent air leaks from the lung parenchyma [24]. Leveraging this strategy for drug delivery offers several advantages over traditional chemotherapeutic regimens, including local drug release at the target site, improved therapeutic efficacy and minimized systemic toxicity, enhanced bioavailability and tissue penetration, and 100% patient compliance (Fig. 1). Additionally, drug release occurs over a prolonged period of time and avoids the requirement of frequent chemotherapy dosing protocols.

Similar strategies show some benefit, either in *in vivo* models and/or in the clinic. For example, Gliadel® wafers of carmustine increase survivability in patients with malignant gliomas from 11.6 to 13.9 months [25]. Intracranial implants of paclitaxel afford higher survival in a rat model of malignant glioma [26]. More recently, hyaluronate-based films loaded with cisplatin prevent tumor recurrence in pleural mesothelioma [27], while cisplatin-loaded superhydrophobic polymer meshes increase recurrence-free survival *in vivo* [28].

Here, we are investigating polymer-coated buttresses to deliver eupenifeldin – a novel anticancer agent (Fig. 1C). Eupenifeldin is a fungal metabolite, first reported in 1993 by researchers at Bristol-Myers Squibb from cultures of *Eupenicillium brefeldianum.* It exhibits potent cytotoxic activity at the nanomolar level against, for example, human MDA-MB-231 breast, MSTO-211H mesothelioma, and OVCAR-3 and OVCAR-8 ovarian cancer cell lines, and *in vivo* activity against a murine model of leukemia [29, 30]. However, eupenifeldin’s physical properties, particularly its poor water solubility, handicap its use as a standalone chemotherapeutic agent. To overcome the poor solubility of eupenifeldin and investigate its potential as a cancer therapeutic against an *in vivo* solid tumor, we report eupenifeldin-loaded polymer-coated surgical buttresses as an extended drug release formulation (Fig. 1B). The prolonged cytotoxic activity of this formulation was evaluated using long-term cell

culture assays, and the efficacy in reducing the recurrence rate of NSCLC was evaluated using a murine model of lung cancer recurrence.

2. Materials and methods

2.1. Materials and instrumentations

Eupenifeldin was isolated and characterized from *Neosetophoma* sp. (strain MSX50044) as reported recently in detail [30]. The purity of eupenifeldin was > 97% as determined by ^{1}H NMR and UPLC analyses (Figs. S1 & S2). Poly(glycerol monostearate co-Ɛ-caprolactone) polymer (PGC-C_{18}) was synthesized as previously described [31].

Phosphate buffered saline (PBS) solution was prepared using 137 mmol/L NaCl (Fisher Scientific), 2.7 mmol/L KCl (Macron Fine Chemicals), 1.8 mmol/L KH_2PO_4 (EMD Millipore Corporation), and 10 mmol/L Na_2HPO_4 (Fisher Scientific). This PBS solution was supplemented with 2% Tween 80 (VWR International) to improve the solubility of eupenifeldin (Fig. S3), and 0.02% of sodium azide (Sigma-Aldrich) to prevent microbial growth. The pH was buffered to 7.35–7.45.

The UV absorbances of standard solutions and PBS samples were measured using an Agilent Cary Ultraviolet-Visible (UV-Vis) Spectrophotometer at a wavelength of 364 nm, which is the λ_{max} of eupenifeldin in PBS solution.

2.2 Preparation of polyglycolic acid (PGA) buttress

Fibrous meshes of polyglycolic acid (PGA) were used as a buttress onto which PGC-C_{18} was coated with or without eupenifeldin. PGA polymer was selected to develop the buttress based upon its unique properties, where PGA polymer is insoluble in most organic solvents, including dichloromethane (Fig. S11) [32]. A large mesh was used for the buttress stock, formed via electrospinning of a 20% wt/v solution of PGA dissolved in hexafluoro-2-propanol, pumped at 25 mL/hr at ~13 kV, and with a tip-to-collector distance of 9 inches. The resulting mesh were ~140 μm in thickness with a mass density of 5.84 g/cm^2. Electrospun PGA buttress exhibited a mean fiber diameter of 3.63 micron and a porosity of 38.05% as determined via image analysis with the ImageJ plugin, DiameterJ. While this is an in-house generated PGA-based buttress, PGA is a biodegradable polymer commonly used in FDA-approved sutures and buttresses (e.g., ~140 μm thickness, 5.84 g/cm^2 basis weight (i.e., density), and 38.05% porosity) as well as drug delivery carriers due to its fast degradation (~ 3 months) [33].

2.3. Preparation of eupenifeldin-polymer loaded buttresses

A sheet of PGA polymer was cut into 1 cm^2 buttresses. These were used to prepare six different formulations of eupenifeldin-loaded buttresses (formulations **1**-**6**). Briefly, PGC-C_{18} polymer (10% w/v) and eupenifeldin (1.0% w/v) were dissolved in dichloromethane to produce a clear eupenifeldin-polymer solution. A second solution of blank polymer (10% w/v) dissolved in dichloromethane was prepared to cover the eupenifeldin-polymer layers in formulations **2**, **4** and **5**, as described below. Unloaded or eupenifeldin-polymer solutions were uniformly coated layer by layer over the upper and lower face of each buttress. Each

layer was created by applying 30 μL of blank polymer solution (~3 mg of PGC-C_{18} polymer) or 30 μL of eupenifeldin-polymer solution (~3 mg of PGC-C_{18} polymer with 300 μg of eupenifeldin) using a Hamilton syringe and spread over the buttress face. Each layer was allowed to dry for at least one hour before adding any subsequent layers. Formulations **1**-**6** differ in the number and types of loaded layers as follows (Fig. 1B): formulation **1** were loaded with a single layer of eupenifeldin-polymer on each face (total of 600 μg of eupenifeldin), formulation **2** was the same as **1** with an additional single layer of unloaded polymer on each face (total of 600 μg of eupenifeldin), formulation **3** was loaded with two layers of eupenifeldin-polymer on each face (total of 1200 μg of eupenifeldin for each), formulations **4** and **5** were the same as **3** with an additional single layer and two layers of unloaded polymer on each face, respectively (total of 1200μg of eupenifeldin). Formulation **6** was four layers of unloaded polymer on each face. These were used as a vehicle control in the *in vitro* and *in vivo* testing. All formulations were placed on glass cover slips and left overnight under nitrogen lines to dry completely. SEM images were taken for unloaded PGA buttress and eupenifeldin-loaded buttresses (formulations **1**-**6**). Once coated and dried, formulations **1**-**6** had a smooth, uniform topology with no exposed PGA fibers (Fig. S5). Table S1 summarizes the number of layers and the composition of eupenifeldin and PGC-C_{18} across formulations **1**-**6**. To further illustrate the layering concept and ensure that formulations **1**-**6** maintain the layered structure as envisioned in Fig. 1, we coated a 1-cm^2 PGA buttress from one side with phycocyanobilin-polymer solution (blue-colored) to create the first and the third layers and ent-shiraiachrome A-polymer solution (red-colored) to build the second and the fourth layers (Fig. S12). Each subsequent layer does not entirely cover the previous layer thereby allowing visualization of all four layers under a microscope (Fig. S12). Phycocyanobilin and ent-shiraiachrome A are colored secondary metabolite with high solubility in DCM (similar to eupenifeldin). The alternate blue/red layers demonstrate that the layers stay intact upon coating and any mixing between them is minimal.

2.4. Release study of eupenifeldin-loaded buttress formulations 1–5

Given the low solubility of eupenifeldin in aqueous media, various steps were taken to ensure the continuous release of eupenifeldin and the accurate measurement of its release profile. These include measuring the solubility of eupenifeldin in phosphate buffer saline (PBS) across a suite of percentages of Tween 80 (Fig. S3). Eupenifeldin solubility greatly increased with the addition of Tween 80 (e.g., 1.7 μg/mL without Tween 80 v. 50 μg/mL with 2% v/v Tween 80; Fig. S3). Moreover, we identified the optimal buffer volume of 50 mL by conducting a volume-saturation study (Fig. S4) in which five buttresses, each loaded with 600 μg of eupenifeldin, were submerged in 20, 50, and 100 mL of release buffer (PBS with 2% v/v Tween 80). Eupenifeldin release was measured for 25 days without changing the buffer. Total eupenifeldin released increased with time and, over 25 days, exceeded 1200 μg in the 100- and 50-mL release buffers (Fig. S4). In contrast, the 20 mL PBS solution was saturated within a week, demonstrating the inadequate solvation capacity of this volume of release buffer. Accordingly, 50 mL of PBS with 2% Tween 80 was used as a release media with an estimated solvation capacity of 2500 μg of eupenifledin.

Each formulation (i.e., **1**-**5**, Fig. 1B) was submerged in 50 mL PBS containing Tween 80 (2% v/v) with a pH range of 7.35–7.45 and incubated at 37 °C for 90 days. At specific time

intervals (Fig. S6), the entire PBS solution was collected and replaced with the same volume of fresh buffer to ensure the continuous monitoring of eupenifeldin release. Collected buffer samples were refrigerated at 4 °C until analysis (~2–3 weeks); a day before analysis, buffer samples were incubated overnight at 37 °C with shaking to ensure homogeneity and that eupenifeldin was fully dissolved. The concentration of eupenifeldin in collected PBS samples was measured by UV-Vis at 364 nm.

2.5. Standards preparation and method validation

Six standard samples of PBS with known eupenifeldin concentration (ranging from 80 ng/mL to 2.56 μg/mL) were prepared to build a calibration curve using a UV-Vis spectrophotometer (λ = 364 nm). All measurements were performed in triplicate (n=3), and a new calibration curve was created each time the PBS samples were analyzed, which was every 2 to 3 weeks (a total of five calibration curves were obtained, Fig. S7). These standard curves were used to determine the amount of eupenifeldin in PBS samples collected from the *in vitro* release study. The linearity of each calibration curve was assessed using linear least squares regression analysis. The correlation coefficient (R^2) in all calibration curves was 0.998 ± 0.001, and the linearity range was 0.08–2.56 μg/mL. The relative error (RE) remained less than or equal to 15.5% over a concentration range of 160 ng/mL to 2.56 μg/mL. The limit of quantitation (LOQ) was 152.0 ± 50.0 ng/mL, which is the lowest amount of analyte that can be quantitatively determined with suitable precision and accuracy. LOQ was defined as 10 S_a / b, where S_a is the standard deviation of the *y*-intercept, and b is the slope of the calibration curve. Relative standard deviation (RSD) and relative error (RE) percentages were calculated to evaluate the precision and accuracy of the calibration curves, as summarized in Table S2 and Fig. S7.

2.6. Extraction of eupenifeldin-loaded buttress formulations 1–5

The amount of eupenifeldin remaining on formulations **1**-**5** was measured by extracting three of the eupenifeldin-loaded buttresses of each formulation, both before being exposed to PBS solution and after 30, 60, and 90 days of being submerged in PBS. At the designated time point, each formulation was dissolved in 1 mL dichloromethane. The polymer was then precipitated from eupenifeldin by adding a 50:50 mixture of water and acetonitrile. After vortexing, the organic layer was separated from the aqueous layer and evaporated to dryness. The remaining eupenifeldin from the dried organic layer was re-dissolved in dimethyl sulfoxide and quantified by UV-Vis.

2.7. Long-term in vitro cytotoxicity assay of eupenifeldin-loaded buttress formulations 1–6

Each buttress in formulations **1**-**6** was placed in a Transwell insert of a 12-well plate and co-incubated with adherent LLC, murine Lewis lung carcinoma, and A549, human lung carcinoma, cells 24 h after plating. Cells were maintained in complete media containing 10% fetal bovine serum and 1% penicillin/streptomycin in DMEM and F-12K media for LLC and A549 cells, respectively. After 24 h of co-incubation, the buttress was transferred into the elution sink (2% v/v Tween 80 in PBS) to allow for continuous eupenifeldin release for 6 days before a second cycle of co-incubation with another aliquot of freshly plated

cancer cells. Eupenifeldin-loaded buttresses were washed in two 50 mL PBS baths prior to placement into the Transwell inserts to remove residual Tween 80. These cycles of co-incubation (24 h) and elution (6 days) were conducted for a total of 10 weeks. The viability of tumor cells was assessed three days after each co-incubation period and compared to those exposed to blank polymer-loaded buttresses (i.e., formulation **6**), which acted as a vehicle control, and a non-treated control with no film. Cell viability was assessed using a tetrazolium-based colorimetric assay of 3-(4,5-dimethylthiazol-2-yl)-5-(3-carboxymethoxyphenyl)-2-(4-sulfophenyl)-2H-tetrazolium (MTS; CellTiter 96® Aqueous One Solution Cell Proliferation Assay).

2.8. In vivo maximum tolerated dose study

Animal studies were approved by the Institutional Animal Care and Use Committee at Massachusetts General Hospital (IACUC approval number is 2019N000085). To determine the maximum tolerated dose (MTD) of “free” eupenifeldin (i.e., not loaded into a buttress), eupenifeldin was solubilized in 50/50 Cremophor EL/ethanol, the excipient used clinically to delivery paclitaxel, due to eupenifeldin’s poor aqueous solubility. Intraperitoneal injections of eupenifeldin were systemically administered to 6- to 8-week old C57Bl/6 mice with predetermined doses of 20 μg, 40 μg, 60 μg, 120 μg, 180 μg and 540 μg of eupenifeldin (Table S3). Animals were monitored daily for clinical deterioration manifested by significant weight loss, lethargy, and/or respiratory distress.

To determine the MTD of eupenifeldin-loaded buttresses, five different doses were employed, all of which used the structure of formulation **5** (Fig. 1B). The amount of eupenifeldin loaded into the 1 cm^2 buttress was tittered to five doses: 1200 μg, 600 μg, 300 μg, 200 μg, or 100 μg. These eupenifeldin-loaded buttresses were implanted subcutaneously on the dorsum of non-tumor-bearing animals. Animal weight (as a corollary of morbidity) and mortality were followed over 14-days. A greater than 20% drop in body weight or severe clinical deterioration (respiratory distress, lethargy, decreased activity) necessitated humane euthanasia.

2.9. In vivo murine model of local cancer recurrence

Six-to-eight-week-old female C57Bl/6 mice were injected subcutaneously at the interscapular space of the upper dorsum with 750,000 LLC cells. Tumors were allowed to grow for approximately two weeks and resected after reaching at least 500 mm^3. Using sterile technique and under isoflurane anesthesia, visible tumor was removed leaving behind adjacent tissue, such that residual microscopic disease leads to recurrent tumor growth. Animals were immediately randomized into treatment groups: (1) surgery only (no treatment implanted), (2) implantation of blank unloaded formulation, and (3) implantation of 100 μg eupenifeldin-loaded formulation. Eupenifeldin formulation was applied directly over the resection bed and secured with suture at the corners. The incision was closed with wound clips. Mice were monitored postoperatively for clinical deterioration, freedom from local recurrence, and survival. Recurrence was determined by the presence of tumor re-growth at the surgical site. Animals were euthanized when tumor size had reached greater than 2 cm, appeared systemically ill, or had nonhealing skin ulcers. A log-rank (Mantel-Cox) test was

used to assess efficacy of the treatments for statistical significance in prolonging tumor-free survival and overall survival.

2.10. Histological analysis

After euthanasia, autopsy was conducted on the animals. Organs and tissue surrounding the buttress implants were harvested and stored in 10% formalin. Tissues were sent to the core facilities for paraffin embedding, sectioning, and H&E staining.

3. Results and Discussion

Given the limited knowledge on the anticancer activity of eupenifeldin, we submitted eupenifeldin for evaluation against the NCI cell line panel representing a total of 60 human tumor cell lines [34]. Eupenifeldin showed the greatest activity against melanoma, leukemia, and lung cancer cell lines (Fig. S8). We are keenly interested in treatments to prevent lung cancer recurrence after a surgical resection and, thus, the broad activity of eupenifeldin drew our interest. However, eupenifeldin is hydrophobic with negligible solubility in water and therefore requires a traditional excipient or drug delivery device to enable *in vivo* delivery. Therefore, to assess the ability of eupenifeldin to eliminate residual malignant disease following tumor resection via a local-delivery system, we developed eupenifeldin-loaded buttresses of various formulations to achieve a sustained, tunable therapeutic dose over a prolonged period. We initially characterized drug release and evaluated the cytotoxicity of the buttresses *in vitro* against two NSCLC cell lines over 70 days. Finally, we determined the maximum tolerated dose *in vivo* and characterized the buttress' ability to prevent local tumor recurrence in a murine model of lung cancer recurrence.

3.1. Kinetics of eupenifeldin release from polyglycolide buttresses

Preventing local lung cancer recurrence following surgical resection of the primary tumor requires a drug-delivery system that can maintain a therapeutic, though non-toxic, dose of the anticancer agent for a prolonged period of time. In particular, the local drug-delivery system should minimize the intensity of initial burst release that usually occurs within the first 24–48 h, so as to avoid interfering with post-surgical healing. To achieve these requirements, PGA buttress was manufactured in-house, and it was coated with five different eupenifeldin-loaded buttresses formulations (**1–5**, Fig. 1B) whose drug-release characteristics were then evaluated. Specifically, we varied the amount of eupenifeldin between 600 and 1200 $\mu g/cm^2$ and the number of unloaded polymer layers covering the eupenifeldin layer. The goal of this study was to evaluate the impact of both total drug loading as well as polymer layering or thickness (e.g., multiple drug loaded- or unloaded polymer-layers) upon eupenifeldin release kinetics. Due to eupenifeldin's hydrophobic character, we selected a biodegradable, biocompatible, hydrophobic polymer, poly(glycerol monostearate co-ε-caprolactone) (PGC-C_{18}) [31], as the coating/encapsulating polymer to entrap eupenifeldin.

3.1.1. Kinetics of eupenifeldin release.—We characterized eupenifeldin release profiles over 90 days (Fig. 2). In formulation **1**, eupenifeldin was loaded directly into a single PGC-C_{18} polymer layered on each face of the buttress (Fig. 1B). In formulation **2**, an

additional layer of unloaded PGC-C_{18} polymer was added on each side of the buttress. We hypothesized that this additional polymer layer would slow the release rate of eupenifeldin. Indeed, the initial release of eupenifeldin in the first 4 h was lower in formulation **2** (17.6 ± 2.8%) than in formulation **1** (34.0 ± 2.2%). We attributed this reduction in release to the extra polymer layer on formulation **2**, which provided an additional barrier to the release of eupenifeldin to the surrounding release medium. After 24 h, the release profiles were similar for both formulation **1** and **2** (Fig. 2A). Over 90 days, 86.5 ± 2.3% of the eupenifeldin payload was released from formulation **1**, while 78.9 ± 1.4% was released from formulation **2** (Fig. 2B). These data correlated well with the mass-balance of eupenifeldin performed by extracting unreleased eupenifeldin from each formulation after 90 days (Fig. 2D).

3.1.2. Impact of layering on kinetics of eupenifeldin release.—Based upon the result that formulation **2** experienced a delay in burst release compared to formulation **1**, we next interrogated our ability to further tune the release profile through the incorporation of additional loaded- and unloaded polymer layers. We prepared formulations **3**-**5** with 1200 μg of eupenifeldin total per buttress. Formulation **3** mimicked formulation **1** but doubled the total drug through addition of a second layer of eupenifeldin/ PGC-C_{18} on each side (Fig. 1B). Formulation **4** mimicked formulation **3** with one layer of unloaded PGC-C_{18} polymer on each face, while formulation **5** included two layers of empty polymer on each face. These additional layers of empty polymer were added to increase the distance eupenifeldin would have to diffuse through the polymer in order to release, thereby reducing the burst release (i.e., amount of released agent over 24 hr). The initial burst release was highest for formulation **3** (22.2 ± 3.2%), lower in formulation **4** (19.1 ± 5.2%), and the lowest in formulation **5** (15.5 ± 0.7%). As anticipated, formulation **5** exhibited the slowest release rate for the first three weeks as compared to formulations **3** and **4** (Fig. 2A–C). Interestingly, after day 21, formulation **5** maintained a *higher* daily release of eupenifeldin, which is attributed to a generally more moderated and sustained release profile (Fig. 2C). As shown in the cumulative release profiles (Fig. 2B), formulation **3** maintained a considerable release rate of eupenifeldin for approximately 35 days before reaching a plateau. Formulations **4** and **5** showed a more prolonged release of eupenifeldin, up to 50 days for formulation **4** and approaching 90 days for formulation **5**. The total amount of released eupenifeldin during the study was similar among formulations **3**, **4**, and **5** at 70 – 80% of the total eupenifeldin payload over the course of the study. As with formulations **1** and **2**, these data correlated well with the mass-balance of eupenifeldin extracted from the buttresses after 90 days (Fig. 2D).

3.1.3. Mass-balance of eupenifeldin-loaded buttress formulations 1–5—To investigate the mass-balance of eupenifeldin during the release study (i.e., released drug + un-released drug = total drug), we extracted and quantified the eupenifeldin remaining in each formulation at predesignated timepoints over the course of the study (Fig. 2D). These results correlated well with the previous eupenifeldin-release data confirming the kinetics of release. By 30 days, formulations **1** and **2** contained no detectable eupenifeldin. Formulation **5** showed the highest amount of remaining eupenifeldin at 30 and 60 days, indicating the slowest release rate amongst formulations **3**–**5**. Overall, only formulations **3**-**5** maintained a measurable eupenifeldin payload after the first 30 days and only formulation **5** contained a

measurable amount of eupenifeldin by 60 days (approximately 50 μg). This remaining drug was released over the final 30 days and no eupenifeldin was detected at the end of the release study. Of note, the recovered eupenifeldin at 0 day accounted for 81–88% of the theoretical loading, which may be attributed to partial loss through the processes of weighing, loading, and extraction. Furthermore, the cumulative released amount of eupenifeldin at 90 days accounted for more than 82% of the originally extracted amount at 0 day of formulations **1**-**5**. The handling of eupenifeldin-loaded buttresses over a period of 90 days may also contribute to this minor loss of mass.

3.2. Long-term cytotoxicity of formulations 1–5 against lung cancer cell lines

Eupenifeldin showed cytotoxicity against murine Lewis lung carcinoma (LLC) and human lung carcinoma (A549) cell lines with IC_{50} values of 8.5 and 123.9 ng/mL, respectively (Fig. S9). We next determined the long-term cytotoxicity of formulations **1**-**5** against lung cancer cells. Formulations **1**-**5** that were co-incubated with cells in a Transwell insert for 24 h exhibited a prolonged cytotoxic effect against LLC cells over various durations (Fig. 3A). Formulations **1** and **2** maintained potent cytotoxic activity over four weeks, while formulations **3**-**5** maintained cytotoxicity for eight weeks, with formulation **5** being the longest lasting (i.e., 10 weeks). Against A549 cells (Fig. 3B), the cytotoxic activity of formulations **1** and **2** diminished after the third week, while formulations **3** and **4** performed well until week 6 and formulation **5** showed prolonged cytotoxicity over seven weeks.

3.3 *In vivo* efficacy and toxicity of eupenifeldin-loaded buttresses

To determine the optimal tolerable dose of eupenifeldin, we first performed two dose-escalation studies in C57Bl/6 mice. To determine the maximum tolerated dose (MTD) of "free" eupenifeldin (i.e., not loaded into a buttress), intraperitoneal injections of 20 μg, 40 μg, 60 μg, 120 μg, 180 μg and 540 μg of eupenifeldin were administered (Table S3). All animals in the 60 μg dose group or higher died within 24 hours of injection of acute toxicity. Only in the group receiving 20 μg did more than 50% of the animals survive to one-week post injection. The NCI definition of MTD requires <10% mortality and, therefore, even a dose as low as 20 μg of eupenifeldin in Cremophor EL/ethanol did not meet the requirements for MTD.

To determine the MTD of eupenifeldin-loaded buttresses, five different doses were employed, all of which used the structure of formulation **5** (Fig. 1B). The structure of formulation **5** was selected as it provided the most extended release profile *in vitro*. The amount of eupenifeldin loaded into the 1 cm^2 buttress was tittered to five doses: 1200 μg, 600 μg, 300 μg, 200 μg, or 100 μg. The 1200 μg (n= 5), 600 μg (n= 3) and 300 μg (n= 4) loaded formulations resulted in the most acute and significant decrease in body weight, leading to rapid mortality with a median overall survival (OS) of 2–3 days (Fig. S10). The majority of animals (3 out of 4) receiving 200 μg loaded formulation also experienced early mortality (median OS of 6 days). However, all mice in the 100 μg group maintained stable body weights and survived to at least 14 days. Therefore, we determined the MTD of eupenifeldin loaded buttresses to be 100 μg and proceeded with this loading for the subsequent efficacy study.

The difference in MTD between the buttress-loaded and “free” (i.e., Cremophor EL/ethanol) versions of eupenifeldin (100 μg vs. <20 μg, respectively) clearly demonstrates the benefits of extended or slow-release drug delivery systems over simple bolus systemic delivery. Due to the fact that the dose of drug in the buttress-loaded group would be at least 5X+ higher than that of the “free” drug control, the Cremophor EL/ethanol control was excluded from the following animal studies as the equivalent 100 μg systemic dose was lethal.

To evaluate the *in vivo* efficacy of eupenifeldin-loaded buttresses in preventing local cancer recurrence, we employed a previously developed and published heterotopic murine model of lung cancer recurrence following surgical resection [35]. Tumors were established by subcutaneous injection of LLC cells on the dorsum of C57Bl/6 mice. Tumors were surgically removed once they reached a size threshold of 500 mm^3. Immediately following resection the mice were randomized, and we applied the following treatments at the resection site: (1) no treatment (i.e. surgery alone, control), (2) unloaded-buttresses (i.e., formulation **6** in Fig. 1B, vehicle control), or (3) 100 μg eupenifeldin-loaded buttresses (experimental) which equates to a dose of ~5 mg/kg. Given the toxicity of eupenifeldin, we chose to not perform an equivalent drug alone control in this study.

Animals receiving surgery alone (n=9) exhibited early recurrence (median recurrence day 8) and mortality [median overall survival (OS)=11 days]. Animals treated with control unloaded-buttress following surgery (n=9) had similar recurrence-free and overall survival rates with a median of 6 days to recurrence and a median OS of 9 days, with animals being sacrificed due to progression of malignant disease. In contrast, tumor recurrence was delayed in animals treated with eupenifeldin-loaded buttresses (n=10) following surgery with a median time to recurrence of 16 days (Fig. 4A) and a median disease-specific survival of 30 days (Fig. 4B). However, 60% of the animals treated with eupenifeldin-loaded buttresses developed skin ulcerations, many of which required euthanasia due to their nonhealing nature and thus overall survival, though statistically significant, decreased (median OS=17 days) (Fig. 4C). Given the absence of ulceration with the unloaded buttresses, we investigated the tissues surrounding the eupenifeldin-loaded buttresses. Histological analysis showed local fat and skin necrosis around the eupenifeldin-loaded buttresses (Fig. 5A). Furthermore, animals receiving buttresses loaded with high-dose eupenifeldin (i.e., 1200 μg) exhibited evidence of cardiac and hepatic toxicity, which likely accounts for the mortality of mice receiving eupenifeldin-loaded buttress of higher doses in the MTD study. This toxicity is absent with implantation of the 100 μg eupenifeldin-loaded buttresses (Figs. 5B & C).

Surgical resection offers the best chance for cure in most early stage cancers [36, 37]. The success of surgical cure relies on achieving negative margins to ensure that all disease, including microscopic tumor, is removed to minimize the risk of recurrence. This procedure is not always feasible for either anatomic or physiologic reasons. In lung cancer, for example, the high-incidence of co-morbidities and compromised lung function often limit the amount of removable lung tissue [38]. Less aggressive surgical approaches, such as wedge- or sublobar-resection, are associated with a higher risk of local and loco-regional cancer recurrence due to the presence of positive surgical margins that can grow after the removal of the primary tumor [39, 40]. Unfortunately, lung cancer patients with local

recurrence are often ineligible for a second resection, leaving only less curative options, such as radiotherapy and/or chemotherapy [41, 42].

There is an ongoing effort to develop new treatment approaches to successfully prevent the local recurrence of lung cancer while averting the toxicity, morbidity, and mortality associated with systemic adjuvant chemotherapy [43]. Drug-loaded surgical buttresses, implanted at the site of resection, are one solution to achieve this goal of maintaining a locally therapeutic concentration of the anticancer agent at the resection margin for an extended period of time while averting systemic toxicity. A significant advantage of this polymer-coated buttress system is its ability to encapsulate and deliver a wide range of therapeutic cargoes, including small molecule natural products with poor solubility that cannot be overcome through traditional (e.g., excipient) or nano-based (e.g., particle or liposomal) formulations. Polymer-coated buttresses can often address these challenges through solvent evaporation casting, heat-melt casting or even microparticulate suspension of the agent, in cases where there is no method to co-solvate the drug and polymer [44, 45]. The hydrophobicity of the loaded anticancer agent, along with the hydrophobicity of polymers used to fabricate the coating on the buttress, both play critical roles in determining the drug release profile from these systems. In previous studies, paclitaxel-loaded PGC-C_{18} delivery systems exhibited a prolonged release behavior for 50 days [46, 47]. Poor water solubility of both paclitaxel and PGC-C_{18} polymer allowed this extended release property. Moreover, a sustained release profile of cisplatin was observed for 90 days by loading cisplatin over superhydrophobic nanofiber meshes [28]. On the other hand, short release behavior was reported for cisplatin when loaded over a non-superhydrophobic polycaprolactone film, where cytotoxic efficacy was noticeable only for the first day of exposure [28].

Polyglycolide (PGA) is a linear aliphatic polyester, known since 1954, used to fabricate synthetic bioresorbable sutures [48]. PGA is readily available, non-toxic, biodegradable, and a thermoplastic polymer, all of which are favorable characteristics for a surgical buttress. We chose to use PGA-based surgical buttresses since the PGA-polymer is insoluble in the hydrophobic organic solvents (e.g., dichloromethane) used to dissolve and apply the eupenifeldin- PGC-C_{18} coatings. PGC-C_{18} is a novel biodegradable polymer which has successfully passed FDA 10999 biocompatibility studies [27, 28]. Cast films of PGC-C_{18} are compliant, and the casting procedure is amenable to varied surfaces, including the soft and flexible cloth-like surgical PGA buttresses [31]. Given the design requirements, the toxicity of the eupenifeldin and its hydrophobicity, we prepared eupenifeldin-loaded buttresses of varying PGC-C_{18} and eupenifeldin/ PGC-C_{18} layers to control and extend the release to greater than 30 days. Adding unloaded layers of PGC-C_{18} on top of the eupenifeldin-loaded layers, as in formulation **5**, effectively slows and extends the release profile to 90 days. Multiple factors are likely responsible for the slower release profile achieved in formulation **5**, including the layer-by-layer loading technique used to develop these eupenifeldin-loaded buttresses, the increased thickness of this formulation, and the higher PGC-C_{18} polymer:drug ratio represented by the external blank polymer layers added to each face.

We employed LLC and A549 cell lines for the *in vitro* cytotoxicity studies, as these cells are representative of an aggressive pro-metastatic murine lung tumor cell line of epidermoid

histology and a cell line derived from a human lung adenocarcinoma [49]. Eupenifeldin-loaded buttresses exhibit a more potent and prolonged cytotoxic activity against the LLC cell line than the A549 cell line (8.5 vs. 123.9 ng/mL, respectively). This result may be related to the mode of action of eupenifeldin rather than the release characteristics of the buttresses. We are currently further investigating this finding given the stark difference in the IC_{50} values.

We evaluated the *in vivo* efficacy of the eupenifeldin-loaded buttresses in a murine model of lung cancer recurrence following surgical resection. Even very low doses (20 μg) of "free" eupenifeldin administered via Cremophor EL/ethanol are lethal and the MTD of free eupenifeldin is likely 10 μg or lower; this toxicity is an obvious concern that is being probed via ongoing studies to modify the structure to enhance potency and/or minimize toxicity. Loading eupenifeldin into buttresses reduces the toxicity, though high doses of (200 μg or greater) are still lethal, leading to acute death in mice. Histological analysis revealed cardiac and hepatic toxicity of the drug at the highest dose tested. Loading of only 100 μg eupenifeldin within the polymer buttress avoided systemic toxicity and afforded a modest, but statistically significant, delay in the time to tumor recurrence and a significant improvement in disease-specific survival. However, the eupenifeldin-loaded buttresses impaired local tissue healing, suggesting another challenge that must be explored in the future. Additional studies focused on the kinetics of delivery and mechanism of action are underway to address this concern. *In vivo* reduction in post-surgical local recurrence of various types of cancer were previously reported using chemotherapy-loaded drug delivery systems, such as cisplatin-loaded polymeric films for pleural mesothelioma [50, 51], paclitaxel-loaded polymer films for NSCLC and sarcoma [46, 47], and doxorubicin-loaded film for neuroblastoma [52]. However, this is the first application of a natural product that is still in the pre-clinical stages of investigations in such a prolonged local delivery system for cancer treatment. This has the added benefit of demonstrating the value of such delivery systems for testing the efficacy of cytotoxic agents that may still have poor physical properties (i.e., prior to further development). Although the translation of such promising *in vitro* and *in vivo* efficacy into clinical settings is highly challenging, investigating optimal delivery platforms is important for clinical applications, both to maximize efficacy and to minimize toxicity. Many major anticancer agents, such as paclitaxel and camptothecin, were fraught with toxicity and solubility challenges early in their development [53], and yet today, they are used as front line chemotherapeutic agents. Notwithstanding the challenges observed with eupenifeldin, given the need for new anticancer agents and the efficacy observed in this murine model of lung cancer recurrence when delivered as a eupenifeldin-loaded buttress, further studies of this anticancer drug lead are warranted.

5. Conclusion

Systemic chemotherapy is not recommended for early stage patients with non-small cell lung cancer due to the unfavorable risk:benefit ratio. Drug-loaded buttresses are a promising drug delivery strategy with significant potential to prevent local tumor recurrence following surgery. Eupenifeldin-loaded buttresses are efficacious *in vitro* for 70 days and delay tumor recurrence and improved disease-specific overall survival in a murine model of resection. From a drug delivery perspective, we describe: 1) the first use of eupenifeldin against any

solid tumor; 2) a delivery system which enables controlled and extended release of an active agent via a layering method; and, 3) long-term *in vitro* cytotoxic activity and *in vivo* decreased local tumor recurrence and increased disease-free survival in a murine lung cancer model. The use of a buttress also offers a strategy to evaluate the *in vivo* efficacy of natural-product derived drug leads at an early stage, as many such compounds, including those that eventually became lifesaving chemotherapeutic agents, such as paclitaxel and the camptothecins (among many others), often suffer from solubility issues. Clinically speaking, chemotherapy-loaded buttresses are an attractive therapeutic approach for reducing tumor recurrence and improving the patient risk to benefit ratio. We envision the use of such buttresses offers a "plus" treatment as its implementation does not require a change in the standard of care or surgical procedure except the replacement of a non-drug loaded buttress with a drug-loaded buttress.

Supplementary Material

Refer to Web version on PubMed Central for supplementary material.

Acknowledgement

This research was supported by the National Institutes of Health (NIH)/National Cancer Institute via grants P01 CA125066, R01 CA227433, and R01 CA232708 and via the NIH Small Business Innovation Research (SBIR) program grants R43 CA213538, R43 CA224739, and R44 CA189215.

Funding

This work was supported by the National Institutes of Health (NIH)/National Cancer Institute [No. P01 CA125066, R01 CA227433, and R01 CA232708] as well as the NIH Small Business Innovation Research (SBIR) program [No. R43 CA213538, R43 CA224739 and R44 CA189215].

REFERENCES

[1]. Centers for Disease Control and Prevention, Expected new cancer cases and deaths in 2020, 2018.

[2]. Siegel RL, Miller KD, Jemal A, Cancer statistics, 2020, CA. Cancer J. Clin, 70 (2020) 7–30.

[3]. Bray F, Ferlay J, Soerjomataram I, Siegel RL, Torre LA, Jemal A, Global cancer statistics 2018: GLOBOCAN estimates of incidence and mortality worldwide for 36 cancers in 185 countries, CA. Cancer J. Clin, 68 (2018) 394–424.

[4]. National Cancer Institute, SEER cancer statistics review (CSR) 1975–2016., 2019.

[5]. Zappa C, Mousa SA, Non-small cell lung cancer: current treatment and future advances, Transl. Lung Cancer Res, 5 (2016) 288–300. [PubMed: 27413711]

[6]. Goldstraw P, Chansky K, Crowley J, Mitchell A, Bolejack V, Giroux D, Kingsbury L, Shemanski L, Stratton K, Rami-Porta R, Asamura H, Eberhardt WEE, Nicholson AG, Groome P, Goldstraw P, Rami-Porta R, Serra Mitjans M, Asamura H, Ball D, Beer DG, Beyruti R, Detterbeck F, Edwards J, Galateau-Salle F, Gleeson F, Huang J, Rusch V, Travis W, Krug L, Kennedy C, McCaughan B, Kim J, Park JS, Kim YT, Kondo H, Krasnik M, Kubota K, Lerut A, Vansteenkiste J, Nackaerts K, Lyons G, Marino M, Marom EM, Erasmus J, Rice D, Swisher S, Van Meerbeeck J, Van Schil P, Nakano T, Hasegawa S, Nicholson AG, Nowak A, Peake M, Rice T, Blackstone E, Rosenzweig K, Ruffini E, Saijo N, Sculier JP, Suzuki K, Tachimori Y, Thomas CF, Tsao MS, Turrisi A, Watanabe H, Wu YL, Wu YL, Baas P, Inai K, Kernstine K, Kindler H, Pass H, Falkson C, Filosso PL, Giaccone G, Kondo K, Lucchi M, Okumura M, Abad Cavaco F, Ansotegui Barrera E, Abal Arca J, Parente Lamelas I, Arnau Obrer A, Guijarro Jorge R, Bascom GK, Blanco Orozco AI, Gonzalez Castro M, Blum MG, Chimondeguy D, Cvijanovic V, Defranchi S, De Olaiz Navarro B, Escobar Campuzano I, Macia Vidueira I, Fernandez Araujo E, Andreo Garcia F, Fong KM, Francisco Corral G, Cerezo Gonzalez S, Freixinet Gilart J, Garcia

Aranguena L, Garcia Barajas S, Girard P, Goksel T, Gonzalez Budino MT, Gonzalez Casaurran G, Gullon Blanco JA, Hernandez Hernandez J, Iglesias Heras M, Hernandez Rodriguez H, Herrero Collantes J, Izquierdo Elena JM, Jakobsen E, Kostas S, Leon Atance P, Nunez Ares A, Liao M, Losanovscky M, Lyons G, Magaroles R, De Esteban Julvez L, Marinan Gorospe M, Melchor Iniguez R, Miravet Sorribes L, Naranjo Gozalo S, Alvarez De Arriba C, Nunez Delgado M, Padilla Alarcon J, Penalver Cuesta JC, Pass H, Pavon Fernandez MJ, Rosenberg M, Sanchez De Cos Escuin JS, Saura Vinuesa A, Strand TE, Subotic D, Terra R, Thomas C, Tournoy K, Velasquez M, Yokoi K, The IASLC lung cancer staging project: Proposals for revision of the TNM stage groupings in the forthcoming (eighth) edition of the TNM Classification for lung cancer, J. Thorac. Oncol, 11 (2016) 39–51. [PubMed: 26762738]

[7]. Sawabata N, Ohta M, Matsumura A, Nakagawa K, Hirano H, Maeda H, Matsuda H, Optimal distance of malignant negative margin in excision of nonsmall cell lung cancer: a multicenter prospective study, Ann. Thorac. Surg, 77 (2004) 415–420. [PubMed: 14759408]

[8]. Predina JD, Keating J, Patel N, Nims S, Singhal S, Clinical implications of positive margins following non-small cell lung cancer surgery, J. Surg. Oncol, 113 (2016) 264–269. [PubMed: 26719121]

[9]. Sawabata N, Maeda H, Matsumura A, Ohta M, Okumura M, Clinical implications of the margin cytology findings and margin/tumor size ratio in patients who underwent pulmonary excision for peripheral non-small cell lung cancer, Surg. Today, 42 (2012) 238–244. [PubMed: 22072149]

[10]. Sasaki H, Suzuki A, Tatematsu T, Shitara M, Hikosaka YU, Okuda K, Moriyama S, Yano M, Fujii Y, Prognosis of recurrent non-small cell lung cancer following complete resection, Oncol. Lett, 7 (2014) 1300. [PubMed: 24944713]

[11]. Arriagada R, Bergman B, Dunant A, Le Chevalier T, Pignon JP, Vansteenkiste J, International G Adjuvant Lung Cancer Trial Collaborative, Cisplatin-based adjuvant chemotherapy in patients with completely resected non-small-cell lung cancer, N. Engl. J. Med, 350 (2004) 351–360. [PubMed: 14736927]

[12]. Winton T, Livingston R, Johnson D, Rigas J, Johnston M, Butts C, Cormier Y, Goss G, Inculet R, Vallieres E, Fry W, Bethune D, Ayoub J, Ding K, Seymour L, Graham B, Tsao M-S, Gandara D, Kesler K, Demmy T, Shepherd F, Vinorelbine plus cisplatin vs. observation in resected non-small-cell lung cancer, N. Engl. J. Med, 352 (2005) 2589–2597. [PubMed: 15972865]

[13]. Chemotherapy in non-small cell lung cancer: a meta-analysis using updated data on individual patients from 52 randomised clinical trials. Non-small cell lung cancer collaborative group., Br. Med. J, 311 (1995) 899–909. [PubMed: 7580546]

[14]. Scagliotti GV, The ALPI trial: the Italian/European experience with adjuvant chemotherapy in resectable non-small lung cancer, Clin. Cancer Res, 11 (2005) 5011s–5016s. [PubMed: 16000605]

[15]. Marcucci F, Berenson R, Corti A, Improving drug uptake and penetration into tumors: current and forthcoming opportunities, Front. Oncol, 3 (2013) 161. [PubMed: 23785671]

[16]. Su J, Chen F, Cryns VL, Messersmith PB, Catechol polymers for pH-responsive, targeted drug delivery to cancer cells, J. Am. Chem. Soc, 133 (2011) 11850–11853. [PubMed: 21751810]

[17]. Colby AH, Oberlies NH, Pearce CJ, Herrera VL, Colson YL, Grinstaff MW, Nanoparticle drug-delivery systems for peritoneal cancers: a case study of the design, characterization and development of the expansile nanoparticle, Wiley Interdiscip. Rev. Nanomed. Nanobiotechnol, 9 (2017) doi:10.1002/wnan.1451.

[18]. Griset AP, Walpole J, Liu R, Gaffey A, Colson YL, Grinstaff MW, Expansile nanoparticles: synthesis, characterization, and *in vivo* efficacy of an acid-responsive polymeric drug delivery system, J. Am. Chem. Soc, 131 (2009) 2469–2471. [PubMed: 19182897]

[19]. Wolinsky JB, Colson YL, Grinstaff MW, Local drug delivery strategies for cancer treatment: gels, nanoparticles, polymeric films, rods, and wafers, J. Control. Release, 159 (2012) 14–26. [PubMed: 22154931]

[20]. Perry J, Chambers A, Spithoff K, Laperriere N, Gliadel wafers in the treatment of malignant glioma: a systematic review, Curr. Oncol, 14 (2007) 189–194. [PubMed: 17938702]

[21]. Mo R, Jiang T, Gu Z, Recent progress in multidrug delivery to cancer cells by liposomes, Nanomedicine (Lond). 9 (2014) 1117–1120. [PubMed: 25118703]

[22]. Dong Y, Eltoukhy AA, Alabi CA, Khan OF, Veiseh O, Dorkin JR, Sirirungruang S, Yin H, Tang BC, Pelet JM, Chen D, Gu Z, Xue Y, Langer R, Anderson DG, Lipid-Like nanomaterials for simultaneous gene expression and silencing *in vivo*, Adv. Healthc. Mater, 3 (2014) 1392–1397. [PubMed: 24623658]

[23]. Gu FX, Karnik R, Wang AZ, Alexis F, Levy-Nissenbaum E, Hong S, Langer RS, Farokhzad OC, Targeted nanoparticles for cancer therapy, Nano Today., 2 (2007) 14–21.

[24]. Ueda K, Localization of air leaks by soap bubble, J. Thorac. Dis, 11 (2019) 1229.

[25]. Attenello FJ, Mukherjee D, Datoo G, McGirt MJ, Bohan E, Weingart JD, Olivi A, Quinones-hinojosa A, Brem H, Use of gliadel (BCNU) wafer in the surgical treatment of malignant glioma: A 10-year institutional experience, Ann. Surg. Oncol, 15 (2008) 2887–2893. [PubMed: 18636295]

[26]. Walter KA, Cahan MA, Gur A, Tyler B, Interstitial taxol delivered from a biodegradable polymer implant against experimental malignant glioma, Cancer Res, 54 (1994) 2207. [PubMed: 7909720]

[27]. Sonvico F, Barbieri S, Colombo P, Mucchino C, Barocelli E, Cantoni AM, Cavazzoni A, Petronini PG, Rusca M, Carbognani P, Ampollini L, Physicochemical and pharmacokinetic properties of polymeric films loaded with cisplatin for the treatment of malignant pleural mesothelioma, J. Thorac. Dis, 10 (2018) 194.

[28]. Kaplan JA, Liu R, Freedman JD, Padera R, Schwartz J, Colson YL, Grinstaff MW, Prevention of lung cancer recurrence using cisplatin-loaded superhydrophobic nanofiber meshes, Biomaterials, 76 (2016) 273–281. [PubMed: 26547283]

[29]. Mayerl F, Gao Q, Huang S, Klohr SE, Matson JA, Gustavson DR, Pirnik DM, Berry RL, Fairchild C, Rose WC, Eupenifeldin, a novel cytotoxic bistropolone from *Eupenicillium brefeldianum*, J. Antibiot, 46 (1993) 1082–1088.

[30]. El-Elimat T, Raja HA, Ayers S, Kurina SJ, Burdette JE, Mattes Z, Sabatelle R, Bacon JW, Colby AH, Grinstaff MW, Pearce CJ, Oberlies NH, Meroterpenoids from *Neosetophoma* sp.: a dioxa[4.3.3]propellane ring system, potent cytotoxicity, and prolific expression, Org. Lett, 21 (2019) 529–534. [PubMed: 30620608]

[31]. Wolinsky JB, Ray WC, Colson YL, Grinstaff MW, Poly(carbonate ester)s based on units of 6-hydroxyhexanoic acid and glycerol, Macromolecules, 40 (2007) 7065–7068.

[32]. Cipurković A, Horozić E, Đonlagić N, Marić S, Saletović M, Ademović Z, Biodegradable Polymers: Production, properties and application in medicine, Technologica Acta, 11 (2018) 25–35.

[33]. Manavitehrani I, Fathi A, Badr H, Daly S, Negahi Shirazi A, Dehghani F, Biomedical applications of biodegradable polyesters, Polymers, 8 (2016) 20.

[34]. Gang S, Charles FB, Christopher WB, Brian DA, Fan M, Integrated metabolome and transcriptome analysis of the NCI60 dataset, BMC Bioinformatics, 12 (2011) S36. [PubMed: 21342567]

[35]. Wolinsky JB, Liu R, Walpole J, Chirieac LR, Colson YL, Grinstaff MW, Prevention of *in vivo* lung tumor growth by prolonged local delivery of hydroxycamptothecin using poly(ester-carbonate)-collagen composites, J. Control. Release, 144 (2010) 280–287. [PubMed: 20184934]

[36]. Lackey A, Donington JS, Surgical management of lung cancer, Semin. Intervent. Radiol, 30 (2013) 133–140. [PubMed: 24436529]

[37]. Dare AJ, Anderson BO, Sullivan R, Pramesh CS, Yip C-H, Ilbawi A, Adewole IF, Badwe RA, Gauvreau CL, Surgical services for cancer care, World Bank Publications, Washington, 2015.

[38]. Allen MS, Darling GE, Pechet TTV, Mitchell JD, Herndon JE, Landreneau RJ, Inculet RI, Jones DR, Meyers BF, Harpole DH, Putnam JB, Rusch VW, Morbidity and mortality of major pulmonary resections in patients with early-stage lung cancer: initial results of the randomized, prospective ACOSOG Z0030 trial, Ann. Thorac. Surg, 81 (2006) 1013–1020. [PubMed: 16488712]

[39]. El-Sherif A, Fernando HC, Santos R, Pettiford B, Luketich JD, Close JM, Landreneau RJ, Margin and local recurrence after sublobar resection of non-small cell lung cancer, Ann. Surg. Oncol, 14 (2007) 2400–2405. [PubMed: 17505859]

[40]. Ginsberg RJ, Rubinstein LV, Randomized trial of lobectomy versus limited resection for T1 N0 non-small cell lung cancer. Lung cancer study group, Ann. Thorac. Surg, 60 (1995) 615–622.

[41]. Ma L, Qiu B, Zhang J, Li QW, Wang B, Zhang XH, Qiang MY, Chen ZL, Guo SP, Liu H, Survival and prognostic factors of non-small cell lung cancer patients with postoperative locoregional recurrence treated with radical radiotherapy, Chin. J. Cancer, 36 (2017) 93. [PubMed: 29228994]

[42]. Guggino G, Doddoli C, Barlesi F, Acri P, Chetaille B, Thomas P, Giudicelli R, Fuentes P, Completion pneumonectomy in cancer patients: experience with 55 cases, Eur. J. Cardiothorac. Surg, 25 (2004) 449–455. [PubMed: 15019677]

[43]. Mahvi DA, Liu R, Grinstaff MW, Colson YL, Raut CP, Local cancer recurrence: the realities, challenges, and opportunities for new therapies, CA. Cancer J. Clin, 68 (2018) 488–505.

[44]. Seca AML, Pinto D, Plant secondary metabolites as anticancer agents: successes in clinical trials and therapeutic application, Int. J. Mol. Sci, 19 (2018) 263.

[45]. Narvekar M, Xue HY, Eoh JY, Wong HL, Nanocarrier for poorly water-soluble anticancer drugs--barriers of translation and solutions, AAPS PharmSciTech, 15 (2014) 822–833. [PubMed: 24687241]

[46]. Liu R, Wolinsky JB, Walpole J, Southard E, Chirieac LR, Grinstaff MW, Colson YL, Prevention of local tumor recurrence following surgery using low-dose chemotherapeutic polymer films, Ann. Surg. Oncol, 17 (2010) 1203–1213. [PubMed: 19957041]

[47]. Liu R, Wolinsky JB, Catalano PJ, Chirieac LR, Wagner AJ, Grinstaff MW, Colson YL, Raut CP, Paclitaxel-eluting polymer film reduces locoregional recurrence and improves survival in a recurrent sarcoma model: a novel investigational therapy, Ann. Surg. Oncol, 19 (2012) 199–206. [PubMed: 21769471]

[48]. Middleton JC, Tipton AJ, Synthetic biodegradable polymers as orthopedic devices, Biomaterials, 21 (2000) 2335–2346. [PubMed: 11055281]

[49]. Kellar A, Egan C, Morris D, Preclinical murine models for lung cancer: clinical trial applications, Biomed. Res. Int, 2015 (2015) 1–17.

[50]. Ampollini L, Sonvico F, Barocelli E, Cavazzoni A, Bilancia R, Mucchino C, Cantoni AM, Carbognani P, Intrapleural polymeric films containing cisplatin for malignant pleural mesothelioma in a rat tumour model: a preliminary study, Eur. J. Cardiothorac. Surg, 37 (2010) 557–565. [PubMed: 19766508]

[51]. Lardinois D, Jung FJ, Opitz I, Rentsch K, Latkoczy C, Vuong V, Varga Z, Rousson V, Günther D, Bodis S, Stahel R, Weder W, Intrapleural topical application of cisplatin with the surgical carrier Vivostat increases the local drug concentration in an immune-competent rat model with malignant pleuromesothelioma, J. Thorac. Cardiov. Surg, 131 (2006) 697–703. [PubMed: 16515926]

[52]. Chiu B, Coburn J, Pilichowska M, Holcroft C, Seib FP, Charest A, Kaplan DL, Surgery combined with controlled-release doxorubicin silk films as a treatment strategy in an orthotopic neuroblastoma mouse model, Br. J. Cancer, 111 (2014) 708–715. [PubMed: 24921912]

[53]. Oberlies NH, Kroll DJ, Camptothecin and taxol: historic achievements in natural products research, J. Nat. Prod, 67 (2004) 129–135. [PubMed: 14987046]

Highlights

- Sustained release of eupenifeldin via polymer-coated surgical buttresses prevents locoregional recurrence of lung cancer.
- Eupenifeldin-loaded buttresses achieve a sustained, tunable therapeutic dose over a prolonged period.
- Eupenifeldin-loaded buttresses decrease local tumor recurrence and increase disease-free survival in an *in vivo* resection model.
- Demonstration of a drug delivery platform technology.

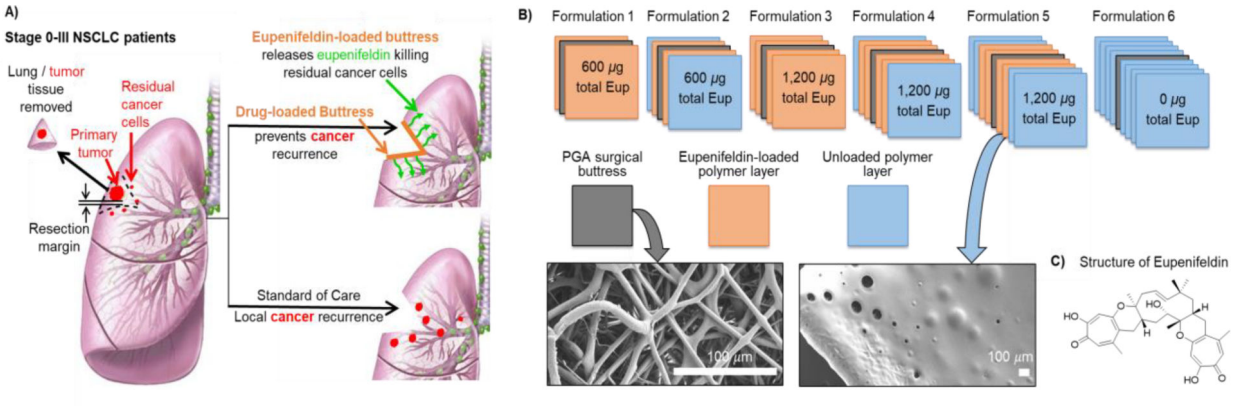

Figure 1.

A. Paradigms of treatment for early stage non-small cell lung cancer (NSCLC) patients: *Bottom path*: unresected residual disease leads to cancer recurrence. *Top path*: drug-loaded surgical buttresses implanted at the resection margin locally deliver drug thereby eliminating residual tumor cells and preventing recurrence. **B.** Schematic illustration of five different eupenifeldin-loaded buttress formulations. Formulation **1**: loaded with 300 μg of eupenifeldin on each face (total of ~600 μg); Formulation **2**: same as **1** with an extra single layer of unloaded polymer on each face (total of ~600 μg of eupenifeldin); Formulation **3**: loaded with 600 μg of eupenifeldin on each face (total of ~1200 μg); Formulation **4**: same as **3** with an extra single layer of unloaded polymer on each face (total of ~1200 μg of eupenifeldin); Formulation **5**: same as **3** with extra two layers of unloaded polymer on each face (total of ~1200 μg of eupenifeldin); and, Formulation **6**: with four unloaded layers of polymer on each face (no eupenifeldin loaded). *Insert:* SEM images of PGA surgical buttress and representative polymer-coated PGA buttress). **C.** Chemical structure of eupenifeldin.

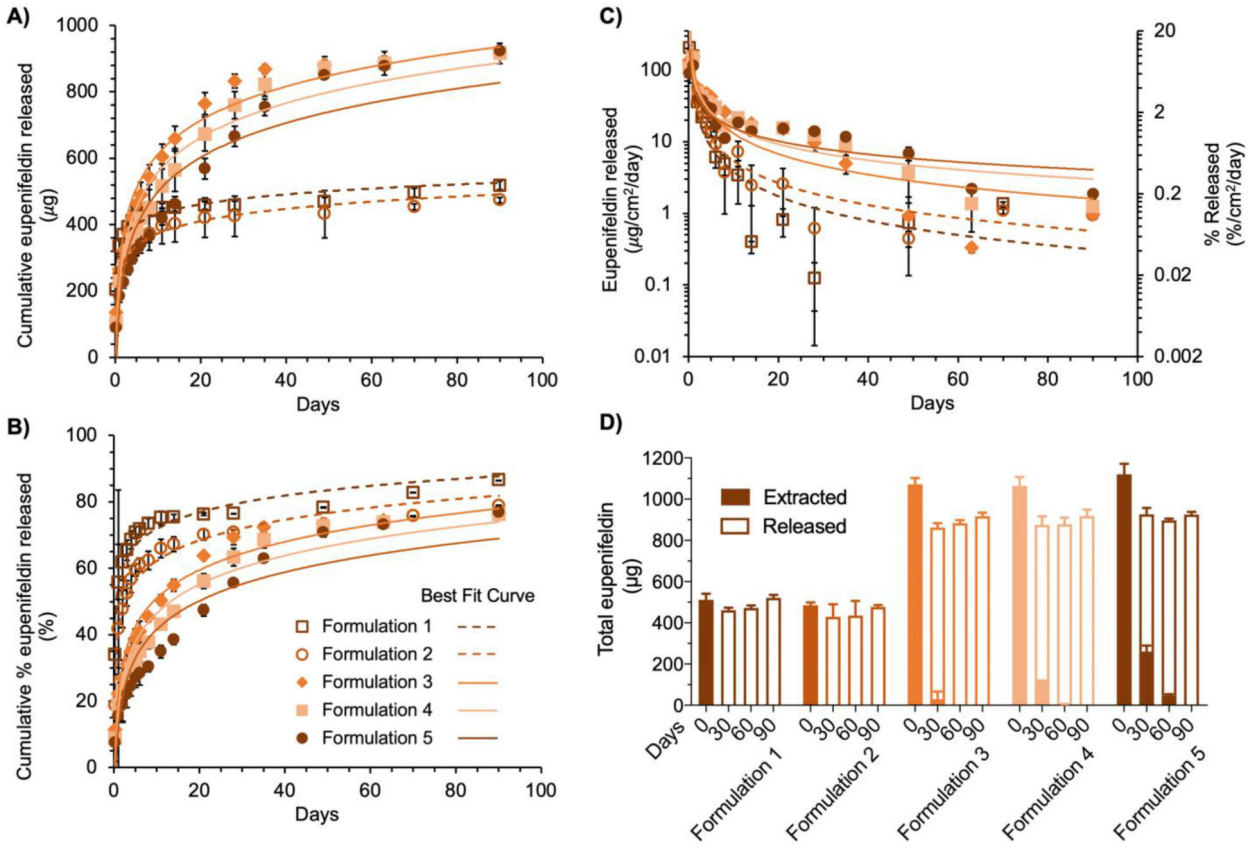

Figure 2.

Kinetics of eupenifeldin release. Cumulative release of eupenifeldin from formulations **1** - **5** over 90 days plotted as mass of eupenifeldin (μg, **A.**) and percent (%, **B.**) of total loaded eupenifeldin in the buttress. **C.** Daily release rate of eupenifeldin normalized by surface area. **D.** Mass-balance of eupenifeldin. Total eupenifeldin is equal to that released plus that remaining (extracted) at each of four time points throughout the release study. For all plots, each time point represents 4–10 experimental replicates. Error bars represent standard deviation.

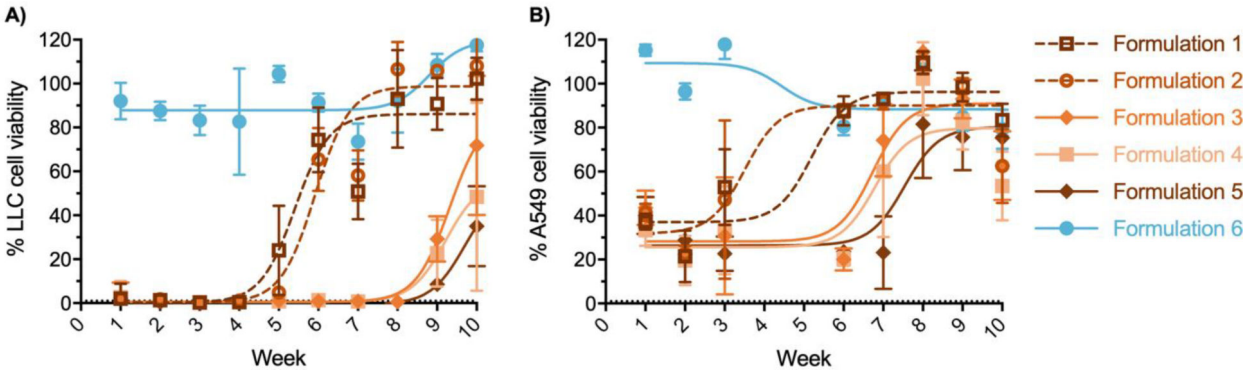

Figure 3.

In vitro cytotoxicity of eupenifeldin-loaded buttresses. Cytotoxicity of formulations **1–5** against Lewis lung carcinoma (**A.**) and human lung carcinoma A549 (**B.**). Each time point represents five replicates. Error bars represent standard deviations.

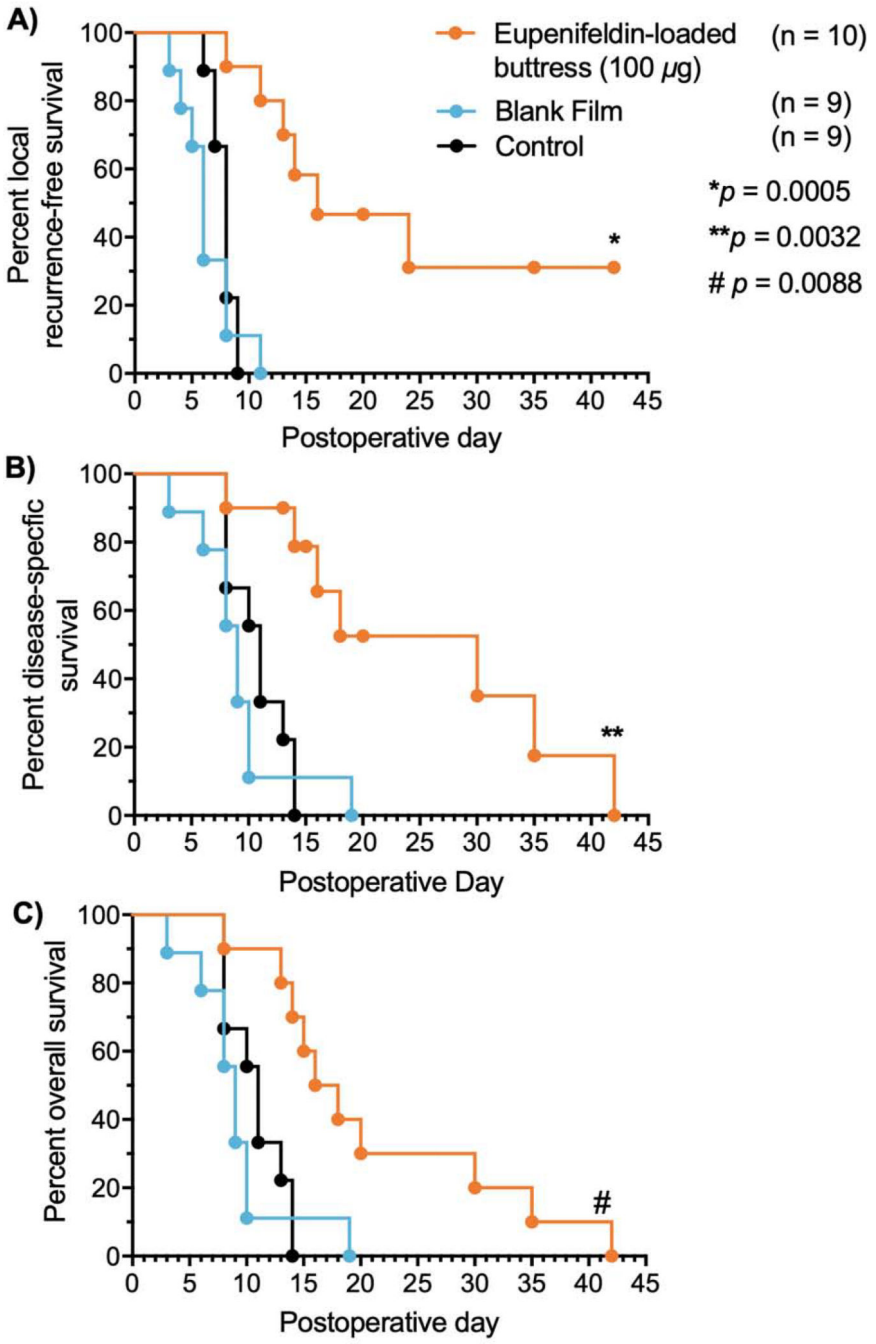

Figure 4.

Local recurrence-free survival (**A.**), disease-specific survival (**B.**), and overall survival (**C.**) after surgical resection of tumors. Disease-specific survival represents animals that died of disease-related reasons only, excluding those that required euthanasia due to reasons unrelated to tumor i.e. nonhealing skin ulcerations.

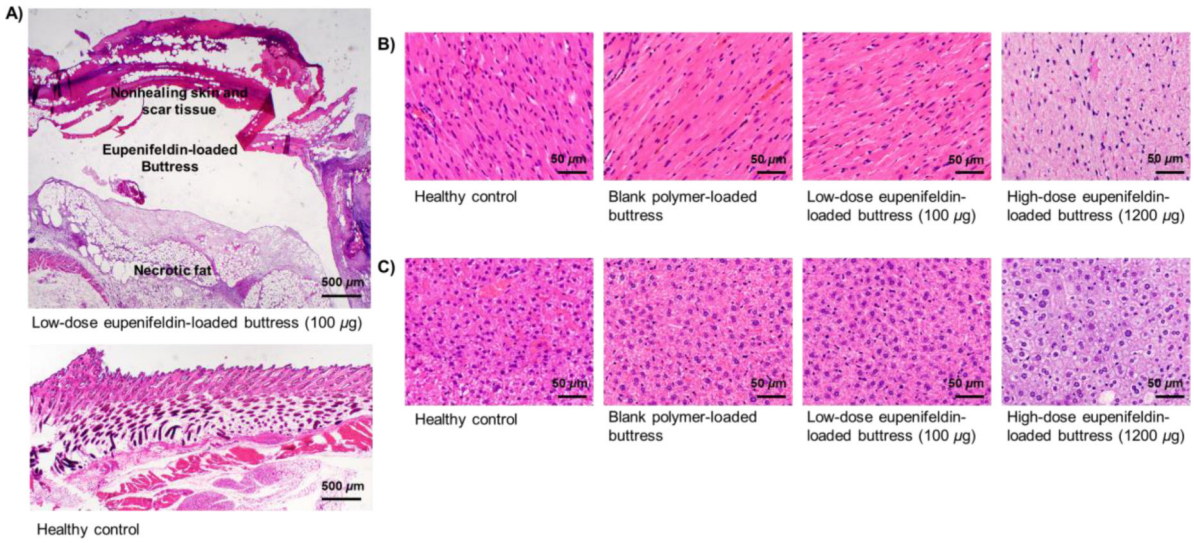

Figure 5.

Tissue necrosis surrounding eupenifeldin-loaded buttress (**A.**). Cardiac (**B.**) and hepatic (**C.**) cells appear vacuolated with irregular appearing cytoplasm in animals treated with high-dose eupenifeldin-loaded buttresses (i.e., 1200 μg), indicative of toxicity.